

THESIS

BENCHMARKING COMPUTATIONS USING THE MONTE CARLO CODE RITRACKS  
WITH DATA FROM A TISSUE EQUIVALENT PROPORTIONAL COUNTER

Submitted by

John Brogan

Department of Environmental and Radiological Health Sciences

In partial fulfillment of the requirements

For the Degree of Master of Science

Colorado State University

Fort Collins, Colorado

Fall 2015

Master's Committee:

Advisor: Thomas B. Borak

Thomas E. Johnson  
Rodney Page

Copyright by John Richard Brogan 2015

All Rights Reserved

## ABSTRACT

### BENCHMARKING COMPUTATIONS USING THE MONTE CARLO CODE RITRACKS WITH DATA FROM A TISSUE EQUIVALENT PROPORTIONAL COUNTER

Understanding the dosimetry for high-energy, heavy ions (HZE), especially within living systems, is complex and requires the use of both experimental and computational methods. Tissue-equivalent proportional counters (TEPCs) have been used experimentally to measure energy deposition in volumes similar in dimension to a mammalian cell. As these experiments begin to include a wider range of ions and energies, considerations to cost, time, and radiation protection are necessary and may limit the extent of these studies. Multiple Monte Carlo computational codes have been created to remediate this problem and serve as a mode of verification for previous experimental methods. One such code, Relativistic-Ion Tracks (RITRACKS), is currently being developed at the NASA Johnson Space center. RITRACKS was designed to describe patterns of ionizations responsible for DNA damage on the molecular scale (nanometers). This study extends RITRACKS version 3.07 into the microdosimetric scale (microns), and compares computational results to previous experimental TEPC data. Energy deposition measurements for 1000 MeV nucleon<sup>-1</sup> Fe ions in a 1 micron spherical target were compared. Different settings within RITRACKS were tested to verify their effects on dose to a target and the resulting energy deposition frequency distribution. The results were then compared to the TEPC data.

## ACKNOWLEDGEMENTS

I would like to thank Dr. Thomas Borak, who took me under his wing and allowed me to join his laboratory here at Colorado State University. His tutelage was invaluable to this project, and I am grateful for the wisdom he has passed to me. I know that my experience with Dr. Borak has given me the tools to become a successful Ph.D. candidate. I will always appreciate his patience with my “biologist” ways, and hope to remain one of the “Boys on the Boat.”

Regarding the Boys, I would also like to thank fellow lab member Rafe McBeth. As both a friend and a colleague, he provided me with advice that helped me when I could not find the answers I was looking for. Apart from the insights he shared with me, our time spent outside of the sciences was equally valuable. I look forward to continuing working together and polishing our basketball skills.

Lastly, I would like to thank everyone else who supported me during this project. The funding, provided by the Mountains and Plains Education and Research Center. The staff and faculty here at CSU in the Health Physics program. My mother and father, Jean and Rick, and my brother, Riley, who were always there for me. My committee members, Drs. Johnson and Page, for their contributions and guidance on this project. My final expression of gratitude goes to Dr. Hatsumi Nagasawa. Had I never met her, I would not be on the path I am on, and my list of accomplishments would be considerably less than they are now.

## TABLE OF CONTENTS

ABSTRACT .....	ii
ACKNOWLEDGEMENTS .....	iii
TABLE OF CONTENTS .....	iv
INTRODUCTION.....	1
MATERIALS AND METHODS .....	10
TEPC .....	10
RITRACKS.....	14
RESULTS.....	21
Total Energy Deposition Simulated by RITRACKS.....	21
Fraction of Expected Dose .....	21
Patterns of Energy Deposition in RITRACKS.....	24
Comparison of RITRACKS and TEPC Patterns of Energy Deposition .....	27
DISCUSSION.....	31
CONCLUSION .....	43
REFERENCES .....	49

## INTRODUCTION

The magnitude of human exposure to high-energy heavy ions (HZE, atomic number  $Z \geq 2$ ) has increased as a manned mission to Mars becomes a reality and the use of such particles for radiation therapy treatments is utilized to a greater extent. Currently, no human data exists to estimate the risk from exposure to HZE particles. Such evaluation requires the use of biological models and understanding of theoretical principles to determine and reduce risks from exposures in radiation mixed fields. A core principle to consider when assessing the quality of radiation damage to biological systems is relative biological effectiveness (RBE).

RBE is a concept used to compare the dose of a test radiation with the dose of 250 kVp (peak kilovoltage) x-rays required to achieve a similar biological outcome, and is defined as the ratio of the absorbed dose of the test radiation to the 250 kVp x-rays (Hall, 1994). The radiobiology of heavy ions has been studied extensively, but there are very few investigations that can provide RBE values for carcinogenic effects (ICRP, 2003). Based on prior studies, it has been observed that there is a wide range of RBE's between different types of radiation. To address this, a radiation weighting factor  $w_r$ , has been defined to apply to an equivalent dose in an organ or tissue. Values for  $w_r$  are specific to the energy and type of radiation incident upon or emitted within the organ or tissue of interest. These values have been designated by the ICRP (ICRP, 1991) and the NCRP (NCRP, 2002). Currently, no weighting factors exist explicitly for HZE ions.

It is known that RBE is influenced by the dose, dose rate, the quality of the radiation, and observed biological outcomes. Zirkle *et al.* specified that biological effectiveness is dependent upon the spatial distribution of the energy imparted and the

density of ionizations per unit pathlength of the ionizing particles (ICRP, 2003). Linear energy transfer (*LET*) was then introduced by Zirkle *et al.* to describe the rate of energy transferred to a target medium per unit distance along a particle's track (Zirkle, et al., 1952). The International Commission on Radiation Units and Measurement (ICRU) initially defined *LET* as

$$LET = - \frac{dE_L}{dx}, \quad (1-1)$$

where  $dE_L$  is the mean energy locally imparted by a particle within the medium and  $dx$  is the distance traversed by the particle through the medium (ICRU, 1968). This original definition quantifies all energy imparted to a maximum radial distance from the primary particle's track or a maximum discrete kinetic energy transfer to a secondary electron and expresses this energy as a single point along the trajectory of the primary ion. By doing this, radial dimensions of the track composed of secondary electrons (delta-rays) possessing considerable amounts of energy are neglected. Using the mean energy imparted also disregards the complexity of the energy deposition distribution as the charged particle traverses along its track through a medium. As a result of these observations, restricted linear energy transfer,  $LET_{\Delta}$ , was established. This concept limited  $dE$  to energy transfers less than a particular value (ICRU, 1968). In most cases, *LET* is found in literature with no specific classification (or subscript) and is assumed to be the unrestricted linear energy transfer.

Another quantity that has been suggested to be more closely related to the biological effect of radiation is lineal energy,  $y$ . It is a microdosimetric quantity defined as

$$y = \frac{\varepsilon}{l}, \quad (2-2)$$

where  $\epsilon$  is the energy imparted by an event within a volume of interest and  $\bar{l}$  is the mean chord length of the volume (ICRU, 1983). The mean chord length of the volume is a result from the random intersection of the region of interest by straight lines (Kellerer, 1971a). The type of randomness of the secants of a convex body is important to consider in this definition. Kellerer described these random intersections under mean free path randomness, or  $\mu$ -randomness.  $\mu$ -randomness was defined such that a chord of a convex body is determined by a point in Euclidian space and a direction, both of which are from independent uniform distributions. For a convex body exposed to a uniform, isotropic field of straight infinite tracks,  $\bar{l}$  is equal to

$$\bar{l} = \frac{4V}{a}, \quad (3-3)$$

where  $V$  is the volume of the body and  $a$  is its surface area (ICRU, 1983). Lineal energy differs from  $LET$  in that it is a stochastic quantity defined by a geometric parameter ( $LET$  is a non-stochastic quantity restricted to energy deposited at a point of interest per unit length of the particle's track). The energy imparted,  $\epsilon$ , within a volume varies per event whereas  $LET$  condenses differential track elements over described distances into one value. This is an important consideration because at subcellular levels, the relevance of stochastic quantities becomes more important (Lindborg, et al., 2013). The drawback to using lineal energy is there are no relationships between mean chord length of a volume and biological action (ICRU, 1983).  $LET$  is still the primary quantity recognized when considering biological damage, making  $LET$  more convenient for established dosimetric calculations. Nevertheless, it is very difficult to directly measure  $LET$  and  $y$  in tissue, calling for the use of experimental models to address the issue.

One of the most widely accepted detectors that fulfill the need to study mixed radiation fields in living tissue is a tissue equivalent proportional counter (TEPC). Currently, TEPCs are being used by NASA as a way to characterize the radiation environment experienced by astronauts in space (for example, the Shuttle-Mir and the International Space Station). The first TEPC was developed by Rossi and Rosenzweig to simulate energy deposited in small volumes of human tissue (Rossi & Rosenzweig, 1955). The proportional counter is surrounded by a tissue equivalent plastic and filled with a gas that provides an energy deposition response similar to human tissue. The gas is set to a low enough pressure that the areal density of the gas in the detector approximates that of a simulated mammalian cell with an appropriate tissue density. An anode wire runs across the diameter of the gas chamber. Most systems employ a helical grid wire surrounding the anode to generate a uniform electric field to prevent any distortions in the electric field when the anode nears the detector wall (the cathode). A TEPC does not directly measure *LET*, it records individual energy deposition events. These events depend on *LET* and the trajectory of a particle through a volume of interest, which in most cases is spherical or cylindrical. The energy deposition is then converted to lineal energy,  $y$ . In studies involving these dimensions, expected values of the probability density functions,  $f(y)$ , and the dose averaged lineal energies are computed. The first moment of  $y$ , the frequency averaged lineal energy,  $\bar{y}_f$ , is determined by (ICRU, 1983)

$$\bar{y}_f = \int yf(y)dy, \quad ( 4-4 )$$

The second moment of  $y$  divided by the first moment, the dose averaged lineal energy,  $\bar{y}_D$ , is determined by (ICRU, 1983)

$$\bar{y}_D = \frac{\overline{y^2}}{\bar{y}} = \frac{\int y^2 f(y) dy}{\int y f(y) dy}, \quad (5-5)$$

The response of a spherical TEPC to HZE ions has been studied extensively (Rademacher, 1997; Rademacher, et al., 1998; Gersey, et al., 2002; Guetersloh, 2003; Guetersloh, et al., 2004; Taddei, 2005; Gersey, 2006; Taddei, et al., 2006). The experiments conducted were unique in that position detectors were included to provide the identity and trajectory of each particle passing through or near the detector. This enabled identification and track reconstruction of every incident ion. Rademacher *et al.* studied TEPC response to  $^{56}\text{Fe}$  ions at  $1050 \text{ MeV nucleon}^{-1}$  where the velocity relative to the speed of light,  $\beta = 0.88$  (Rademacher, 1997; Rademacher, et al., 1998). Gersey *et al.* expanded on TEPC response to  $^{56}\text{Fe}$  ions by observing a range of energies from 200 to  $1000 \text{ MeV nucleon}^{-1}$  where the velocity varied from  $\beta = 0.57$  to  $\beta = 0.87$  (Gersey, et al., 2002; Gersey, 2006). Guetersloh *et al.* reported a comparison of TEPC response to  $^{14}\text{N}$ ,  $^{16}\text{O}$ ,  $^{20}\text{Ne}$ , and  $^{28}\text{Si}$  ions with different energies but analogous *LET* at  $44 \pm 2 \text{ keV } \mu\text{m}^{-1}$  (Guetersloh, 2003; Guetersloh, et al., 2004). Taddei *et al.* extended the above experiment by creating two different energy groups and simulating two TEPC volume sizes. The first group consisted of  $^{12}\text{C}$ ,  $^{16}\text{O}$ ,  $^{28}\text{Si}$ , and  $^{56}\text{Fe}$  at  $376 \pm 15 \text{ MeV nucleon}^{-1}$  ( $\beta = 0.7$ ) and was simulated in a volume having a diameter of  $1 \mu\text{m}$ . The second group was comprised of  $^{12}\text{C}$  and  $^4\text{He}$  at  $220 \pm 7 \text{ MeV nucleon}^{-1}$  ( $\beta = 0.59$ ) and was simulated in a volume having a diameter of  $3 \mu\text{m}$ .  $^{12}\text{C}$  served as the link between the two energy groups' results (Taddei, 2005; Taddei, et al., 2006). The cumulative observations of TEPC response to these experimental conditions follow.

It was observed that approximately 80% of expected *LET* (based on TEPC energy response and simulated diameter) was recorded for incident ions with an impact

parameter of zero in a thick-walled detector (2.54 mm). Impact parameter ( $b$ ) is defined as the radial distance from the center of the TEPC, i.e. ions traversing through the center of the detector equates to  $b = 0$  and the chord length is equal to the diameter of the TEPC. Events with  $b = 0$  display this detriment because the delta-rays generated along the ion's track possess enough energy to escape the sensitive volume and forward moving delta-rays were unable to provide complete energy compensation. As  $b$  increased, energy deposition response became larger than what was predicted based on expected *LET* for that corresponding chord length. When  $b$  was approximately equal to the radius of the gas cavity, an appreciable number of delta-rays were produced within the wall of the cavity and deposited energy within the detector, yielding enhanced energy deposition. As  $b$  became larger than the radius of the sensitive cavity and the trajectory of the primary ion's distance increased from the interface of the sensitive cavity and the wall, contribution to energy deposition from delta rays produced in the wall decreased. The energy deposition by the delta rays was suppressed because absorption of delta rays in the wall of the detector depends upon the wall thickness and the penetration range of the maximum energy delta ray. If the maximum energy was not large enough to penetrate through the wall to reach the detector, deposition of energy in the sensitive cavity by electrons would not occur. A category of sizeable energy deposition events also occurred when incident ions struck the anode wire or helical grid. Overall, Approximately 80% of the expected dose for a uniform beam was observed when only including events when  $b$  was less than the radius of the sensitive volume, i.e. the primary ions possessing a trajectory outside of the sensitive volume were excluded from the absorbed dose calculation. The TEPC correctly measured

absorbed dose for uniform beams of specific ions when all events occurring inside and contributions from outside the sensitive volume were included in the detector response. Charge particle equilibrium was also achieved when all events were included in the measurement of absorbed dose. While recording real-time events of HZE particles interacting with simulated tissue is an ideal approach to investigate the interactions of these radiations with biological systems, these experiments require special considerations to cost, time, and radiation protection. Therefore, it can be advantageous to computationally simulate these same analyses.

Radiation track structure simulations have been used in a variety of projects to study energy deposition events in biomolecular systems (Goodhead & Nikjoo, 1989; Nikjoo, et al., 1997; Cucinotta, et al., 2000; Dingfelder, 2006; Ballarini, et al., 2008). Many radiation-induced phenomena depend on the spatial distribution of discrete energy transfers from the ionizing particle to the irradiated medium, and the patterns of these energy depositions are extremely complex. The interaction mechanisms of radiation with matter are stochastic in nature, leading to most computational models being based on the Monte Carlo method. This statistical approach relies upon repeated random sampling to estimate a quantity that cannot be evaluated deterministically. Numerous computer codes have been developed with the intention of simulating complex experiments.

One of these established codes, the Geant4 toolkit, was used to compare Monte Carlo results with experimental data gathered by a TEPC (Taddei, et al., 2008). Simulations and measurements were generated to record the energy deposition and trajectory for ions ranging from  $^4\text{He}$  to  $^{56}\text{Fe}$  and energies from 200 to 1000 MeV

nucleon<sup>-1</sup>. The results showed that the frequency averaged lineal energy and dose mean lineal energy calculated using Geant4 were within 8% of the measured TEPC data. It should be noted that varying delta-ray range cut values were incorporated in the study. If the electron's range was less than this cutoff, all of its energy was deposited locally.

Another Monte Carlo code that is similar to Geant4 in terms of capacity to simulate HZE radiation track structure is RITRACKS (Plant & Cucinotta, 2010). RITRACKS (Relativistic Ion TRACKS) is currently being developed at the NASA Johnson Space Center by Dr. Ianik Plante. This code has the capability to generate the initial energy and angular distribution of electrons produced by HZE particles traversing through liquid water. Every ion and secondary electron is transported by simulating all interactions within the medium and the position of each radiolytic species is also calculated. The program has been applied to describe patterns of ionization responsible for DNA damage on the molecular scale. Recently, RITRACKS v3.07 incorporated Periodic Boundary Conditions (PBC) to help compensate for high-energy delta rays that escape the simulated irradiated volume and subsequently decrease dose calculations.

The work presented here is an analysis of this code. The objectives of this study focus on benchmarking RITRACKS v3.07 with data acquired from previous TEPC experiments. RITRACKS was originally designed to provide insight on HZE track structure and interactions on the scale of nanometers. The experiments here extend the reach of this program into the microdosimetry range by computing patterns of energy deposition in spherical volumes similar to that of a mammalian cell nucleus. The aim is

to compare simulated dose to a target by RITRACKS to expected dose to a target based on charged particle equilibrium, and contrast the energy deposition distributions from RITRACKS within simulated targets to distributions from a previous TEPC experiment. Data outputs from RITRACKS simulations were normalized when compared to TEPC data due to the fluence differences between the RITRACKS and TEPC experiments. An examination of the PBC was conducted to observe if it was able to accurately reproduce the delta-ray build up required to establish electronic equilibrium and provide a more accurate estimation of dose. Lastly, a comparison of a homogenous system to a heterogeneous system (the target possess a lower density than the surrounding medium) was performed to check if the patterns of energy deposition observed in the TEPC were a result of the incident particles experiencing density changes along their pathlength through the detector.

## MATERIALS AND METHODS

### TEPC

A TEPC is a gas proportional counter that functions by measuring the energy deposited within the tissue-equivalent gas of the detector. The data utilized in this study came from Rademacher *et al.* (Rademacher, 1997; Rademacher, et al., 1998). The TEPC used was spherical, with a sensitive volume diameter of 12.7 mm and a wall thickness of 2.54 mm. The detector can be used to simulate energy deposition within volumes similar in dimension to that of a mammalian cell nucleus by taking advantage of the relationship between media density and diameter, and the pressure of the gas within the TEPC. When the energy loss of passing charged particles in a tissue sphere and a gas sphere with equivalent trajectories for a tissue sphere of diameter  $d_t$  and a gas sphere of diameter  $d_g$  is the same, a conditional simulation can be applied such that

$$\Delta E_t = \left(\frac{S}{\rho}\right)_t \rho_t d_t = \left(\frac{S}{\rho}\right)_g \rho_g d_g = \Delta E_g, \quad (2-1)$$

where  $\Delta E_t$  and  $\Delta E_g$  are the mean energy losses from the charged particle in tissue and gas and  $(S/\rho)_t$  and  $(S/\rho)_g$  are the mass stopping powers of the tissue and gas and  $\rho_t$  and  $\rho_g$  are the densities of the tissue and gas, respectively (ICRU, 1983). If the stopping powers are equal and the atomic compositions are similar between the tissue and gas, the following relationship used to calculate the simulated tissue diameter for a TEPC simplifies to

$$\rho_t d_t = \rho_g d_g. \quad (2-2)$$

Using this formula, the gas within the TEPC can be set to a pressure and corresponding density yielding physical parameters that will allow simulation of a tissue diameter of 1

μm. Because the TEPC used in the previous experiments possessed similar media compositions and density thicknesses of living tissue, it retained analogous ionization cross sections and energy transfer characteristics of a mammalian cell nucleus.

The response of a TEPC is an approximation based on the *LET* of the incident ion, where

$$\varepsilon = LET \cdot x, \quad ( 2-3 )$$

$\varepsilon$  is the energy deposition and  $x$  is the trajectory or pathlength of the ion through the volume. The signal generated is proportional to the ionization events in the gas cavity. The events registered by the TEPC are subject to four types of wall effects seen in simulated small volumes (Rossi, 1967; Oldenburg & Booz, 1970; Kellerer, 1971a; Kellerer, 1971b; Kellerer, 1971c; ICRU, 1983). The effects are: the “delta-ray effect,” the “re-entry effect,” the “V-effect,” and the “scattering effect.” The “delta-ray effect” results if one or more delta-rays produced in the wall of the detector enter the gas cavity. The effect can take place even when the incident charged particle does not travel through the sensitive volume. The “re-entry effect” occurs when a delta-ray exits the sensitive gas cavity and its trajectory is redirected within the wall such that its track re-enters the gas cavity. The “V-effect” arises from an incident charged particle interacting with an atomic nucleus in the wall of the detector, generating two or more nuclear fragments that enter the gas cavity. The last effect, the “scattering effect,” occurs when a primary uncharged particle interacts with the wall and causes two or more charged particles to enter the gas cavity. More than one of these effects could occur in a single recorded event by the TEPC. The most commonly occurring are the delta-ray effect and the V-effect. The energy deposition distribution used from

Rademacher *et al.* was subject to these effects. To eliminate the events resulting from these effects and obtain an energy distribution comprised of Fe interactions with the TEPC only, Rademacher *et al.* utilized a sequence of trigger detectors and positional devices in the experimental setup. Data analysis involved evaluating energy deposited in the sequence of these detectors and devices. Data was recorded on an event by event basis, so the positional devices could be used to determine particle species along the beamline. Signals in the trigger detectors were normally distributed about the expected mean value corresponding to the energy loss of Fe. Events beyond this value  $\pm 3\sigma$  of the mean in the trigger detectors were rejected from analysis.

Figure 2-1 shows the response of the spherical TEPC for a uniform plane parallel beam of  $1000 \text{ MeV nucleon}^{-1}$  Fe particles. To understand each portion of the response, the energy deposition distribution has been separated into three regions A, B, and C, as seen in the figure. This illustration approach has previously been shown by Gersey *et al.*

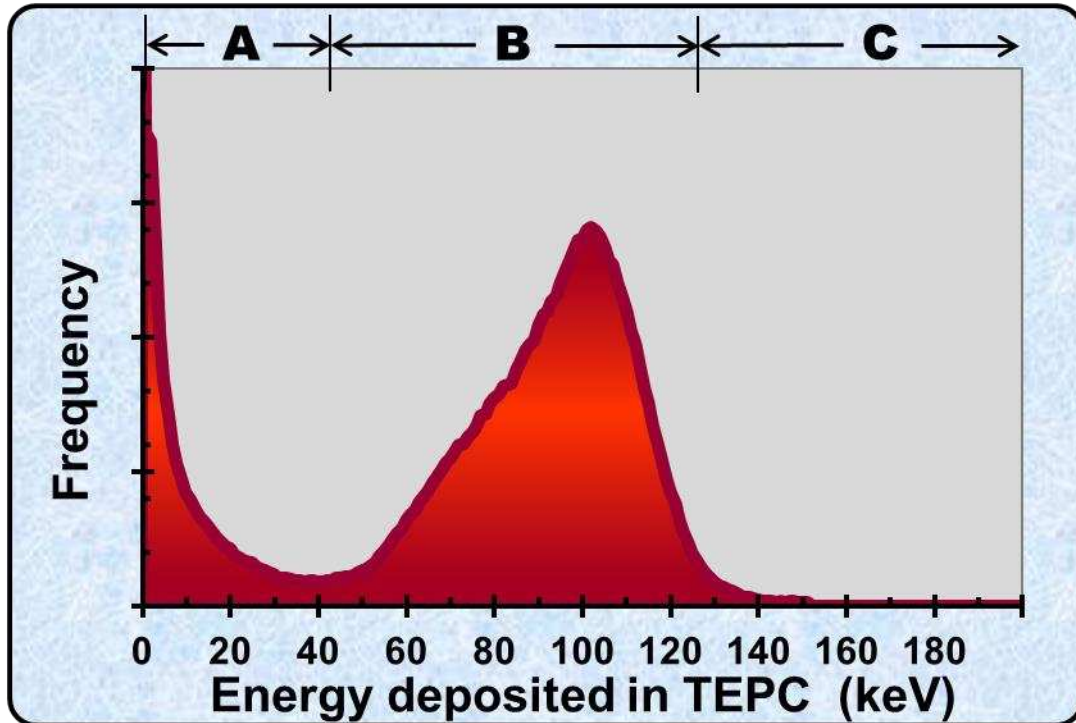


**Figure 2-1.** Probability density distribution (i.e. Response Function) of energy deposited in the TEPC by a uniform beam of Fe particles at  $1000 \text{ MeV nucleon}^{-1}$ . Three regions of energy deposition are indicated as A, B, and C.

Region A contains events where the incident ion misses the gas cavity but passes through the wall of the detector, producing delta-rays that penetrate the sensitive gas cavity. Events in region B correspond to ions that pass directly through the gas cavity. Ions in this region lose some energy deposition when their delta rays escape the cavity and deposit energy within the wall of the TEPC. Some of this loss is compensated by delta-rays produced by interactions of the primary ion in both the proximal and distal halves of the wall of the detector. Region C corresponds to events where the incident ion skimmed the inside wall of the gas cavity or directly hit the anode or helical grid wires within the sensitive cavity. These interactions produced a significant amount of delta-rays and deposited large amounts of energy within the gas.

## *RITRACKS*

The Monte Carlo code RITRACKS version 3.07 was used to generate all of the computational data in this study. The code simulates heavy ion and delta ray tracks using ionization and excitation cross-sections for liquid water. As stated previously, the code RITRACKS utilizes the Monte Carlo method to perform particle transport simulations. The Monte Carlo method is a computational algorithm that utilizes repeated random sampling to obtain an approximate numerical solution. According to the law of large numbers, the average value (or sample mean) from the results of repeated random sampling for large number of trials should be close to the expected value of a given distribution. When applied to particle transport, the general process is: a particle originates at a given point in space with a specified energy and direction, and the particle traverses some distance based on a Probability Density Function (*PDF*) until a “collision” event occurs. The resulting physical interaction that occurs, i.e. absorption or generation of a secondary electron, is again determined by another *PDF*. A separate *PDF* is applied to determine the energy and trajectory of the final products of the “collision” event. This general process repeats until the particle(s) have transferred all of their energy to the medium or have escaped the volume of interest.

Currently, there are two different approaches applied to the transport process: a condensed history approach or a detailed history (full Monte Carlo) approach. The condensed history approach was developed to overcome the computationally labor-intensive process of numerically evaluating the stochastic nature of radiation interactions with matter. In macroscopic scenarios, explicit calculations of every interaction between all secondary electrons produced in a simulation become

unnecessary or impossible. Within these relatively large-scale simulations, a significant fraction of the secondary electrons produced do not affect the outcome of the simulation. Under certain conditions, mean values are sufficient enough to describe energy deposition. This process can also be applied to heavy ions. Examples of codes that utilize this approach are MCNP (Monte Carlo N-Particle transport code) and EGSnrc (Electron Gamma Shower).

A full Monte Carlo approach is ideal for microscopic applications, where every single interaction involved in the simulation is explicitly calculated. In the acceptable scenarios tested by condensed history codes, the variance in energy deposition is small and mean values provide sufficient descriptions of energy deposition. For small volumes and single charged ions, the stochastic nature of energy deposition becomes more important and makes mean values less meaningful. Conversely, RITRACKS is a full Monte Carlo code and follows the particle of interest event by event, computing all ionizations and excitations produced within a simulated liquid medium. The code records the position of any generated radiolytic species as well as the energy and direction of all secondary electrons. The transport process of a given particle consists of all of these successful interactions occurring between the particle and the elements of the liquid medium.

The code functions by defining both an irradiation volume and a target volume within the simulation. The irradiation volume serves as the source of the incident radiation, where the ion tracks originate normal to the flat surface of the volume, as seen in Figure 2-2.

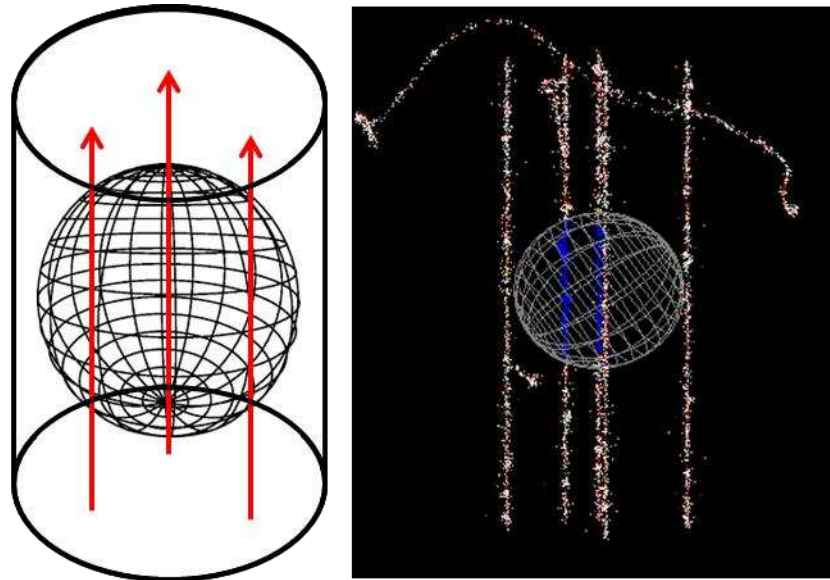


**Figure 2-2.** A depiction of a typical RITRACKS simulation (*left*) and a picture taken from an actual RITRACKS simulation using its built in visualization system (*right*). The red arrows represent the primary ion path traversing through the spherical target from one end to the other of the cylindrical irradiation volume. Blue portions of the track in the image on the right indicate regions of the target intersected by the primary ion and are recorded as energy deposition events. Delta rays produced by the ion can also be seen.

The following description depicts how RITRACKS operates during a given simulation:

As the primary particle traverses through the medium, its trajectory and all interactions are followed. The primary particle is tracked until it exits the irradiation volume, the energy of the particle has decreased below a threshold set by RITRACKS, or it has transferred all of its energy through a physical process. The trajectories and interactions of the generated secondary particles are also followed in this manner, with the exception that the secondary particle is tracked even if it exits the irradiation volume. A target is placed within the irradiation volume, and any interactions that take place within this target are recorded as energy deposition events in units of electron-volts (eV). The output of the simulation is given as total energy deposited within the target per incident particle i.e. if a heavy ion is simulated and produces secondary electrons

that intersect the target, the energy output is a sum of both the primary heavy ion and all secondary electrons' energy deposition events within the target.

Administration of RITRACKS is conducted using a Graphic User Interface (GUI). An electron or various ions spanning from  $^1\text{H}$  to  $^{58}\text{Ni}$  can be selected for simulation (Note: certain isotopes of these elements are also available). The energy for the primary ion is manually entered and an approximate LET is calculated. The irradiation volume can be cylindrical or rectangular in shape, and its dimensions and density are manually entered. The geometric shape of the target can be either spherical or cylindrical. The characteristics of the target (height, diameter, number of targets, and target density), the orientation of the target, and the position of the target within the irradiation volume are also selected by the user. Total number of particles per history is also designated manually, where a history is considered all events taking place within that particular simulation under the parameters entered in RITRACKS. Lastly, boundary conditions for the irradiation volume are set according to the boundaries of the experiment. There are three conditions to choose from: Infinite, Clip, and Periodic Boundary Control (PBC). An Infinite Boundary corresponds to no limitations for pathlengths of a secondary particle, meaning once the particle exits the irradiation volume it continues along its path until it has transferred enough energy to the threshold where it is no longer computed by RITRACKS. Under this boundary, the primary ion is still terminated once it reaches the opposite end of the volume. The Clip Boundary option causes the track of the ion to be "clipped" once the secondary particles have reached the surface of the irradiation volume. Basically, if a secondary electron intersects the volume surface, its track is stopped at that intersection and no more calculations are conducted by the code for that

particular particle. The Periodic Boundary corresponds to a condition where no secondary particle “escapes” the irradiation volume. Any secondary electron that reaches the surface of the volume appears on the opposite side of the volume with the same velocity and trajectory, as seen in Figure 2-3. This “cycle” continues until the particle has deposited all of its energy within the irradiation volume.

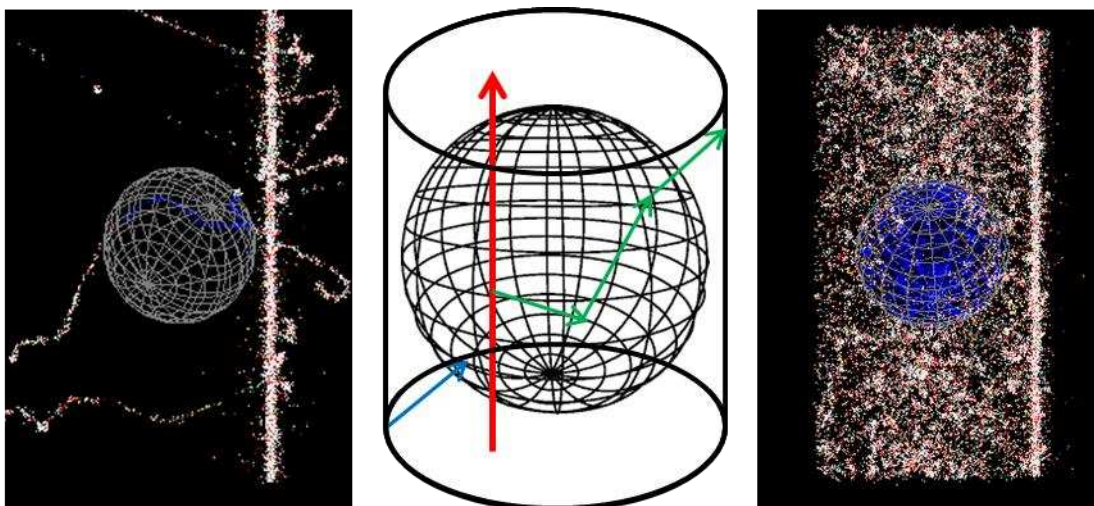


**Figure 2-3.** Rendering of what occurs under PBC (*center*) and two separate simulations visualized by RITRACKS for Fe at 1000 MeV nucleon<sup>-1</sup> (*left, right*). The primary ion is indicated by the red arrow. The green arrow represents a delta ray that possesses enough energy to reach the cylindrical irradiation volume boundary. The blue arrow is the subsequent “re-entry” of that same delta ray. The two outside images show the simulation under the Infinite Boundary setting (*left*), and the Periodic Boundary setting (*right*).

The following section will cover the parameters and settings used in RITRACKS v3.07 for this study. The particle of interest was <sup>56</sup>Fe with an energy of 1000 MeV nucleon<sup>-1</sup>, which corresponds to an approximate LET of 150 keV μm<sup>-1</sup>. This was the same heavy ion and approximately the same energy used in the data from the previous TEPC experiments. The target used in every simulation was spherical with a 1 micron diameter. The irradiation volume was cylindrical with a length of 3 microns. Simulations

were conducted at irradiation volume diameters of 1, 1.05, 1.225, and 1.414 micron(s) to test how dimensions of the irradiation volume and resulting track structure would affect both the dose to the target and the energy deposition distribution. A depiction of this can be seen in Figure 2-4. When the irradiation volume diameter equaled the diameter of the target volume (1  $\mu\text{m}$ ), 100% of the primary ions are expected to directly interact with the spherical target. At an irradiation volume diameter of 1.05  $\mu\text{m}$ , 90% are expected to directly interact. At 1.225 and 1.414  $\mu\text{m}$ , 66.7% and 50% are expected, respectively.

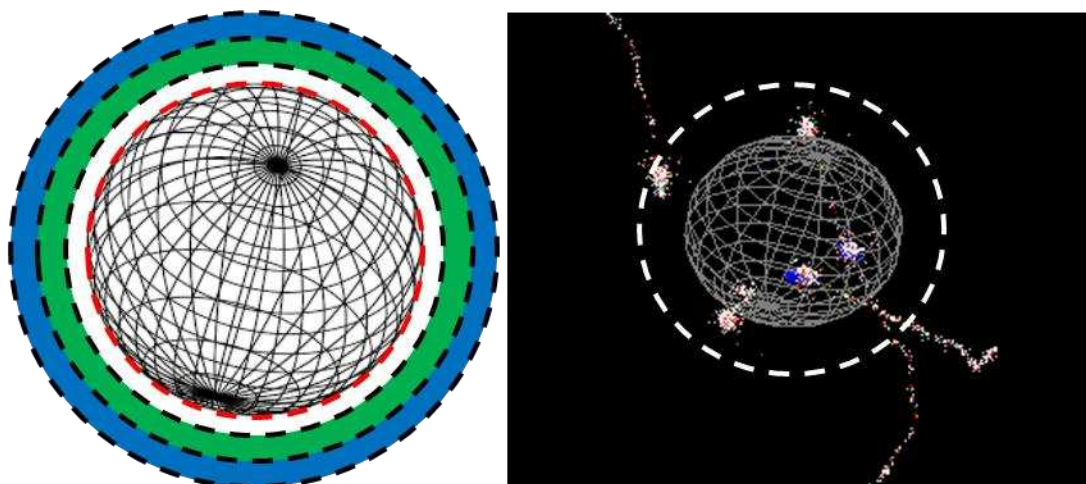


**Figure 2-4.** Drawing of expanding irradiation volume diameter parameter (*left*) and a visualization using RITRACKS (*right*). The dashed red line indicates the simulation where the volume and target diameters are both 1 micron. The expansions to volume diameters of 1.05 (white region), 1.225 (green region), and 1.414 (blue region) microns can also be seen. The visualization in RITRACKS shows a volume diameter of 1.414 microns from a beam's eye view for Fe ions at  $1000 \text{ MeV nucleon}^{-1}$ . Delta rays produced in the medium or target are present.

Total number of particles per simulation for these diameters was 15000, 16500, 22500, and 30000, respectively. With these settings, uniform particle fluence for the entire experiment was achieved. The Infinite and PBC boundaries were used to also test how

these parameters affected dose to the target and patterns of energy deposition under the four irradiation volume diameters listed. The center of the target was located at the center of the irradiation volume. That is, the spherical target is centered within the cylindrical irradiation volume. Two different density systems were tested, designated as either homogenous or heterogeneous. For the homogenous case, the density of the target matched that of the medium surrounding the sphere:  $1 \text{ gram cm}^{-3}$ . In the heterogeneous case, the target density was one tenth of the density of the medium ( $0.1 \text{ gram cm}^{-3}$  and  $1 \text{ gram cm}^{-3}$ , respectively). Using these target parameters ensured the RITRACKS simulation approximated the ionization cross sections and energy transfer characteristics seen in the TEPC experiments as well as stay within the capabilities of RITRACKS.

## RESULTS

### *Total Energy Deposition Simulated by RITRACKS*

The total energy deposited in the spherical target, in kiloelectron volts (keV), calculated from RITRACKS under the experimental parameters listed in Section II: Materials and Methods, can be seen in Table 3-1. Under the Infinite Boundary setting in the homogenous system, the total energy deposited within the sphere does not significantly change among different irradiation volume diameters. A trend can be seen with the Periodic Boundary setting (PBC), where the total energy deposited within the sphere increases as the irradiation volume diameter becomes larger. In the heterogeneous system, the total energy deposited within the sphere increases as the irradiation volume diameter becomes larger under both boundary settings.

Table 3-1. Total Energy Deposited in Spherical Target (keV)

Irradiation Volume diameter ( $\mu\text{m}$ )	Homogenous		Heterogeneous	
	Infinite Boundary	PBC Boundary	Infinite Boundary	PBC Boundary
d = 1.0	1.04E+06	1.40E+06	1.09E+05	1.61E+05
d = 1.05	1.05E+06	1.42E+06	1.14E+05	1.67E+05
d = 1.225	1.07E+06	1.46E+06	1.18E+05	1.77E+05
d = 1.414	1.06E+06	1.49E+06	1.20E+05	1.86E+05

### *Fraction of Expected Dose*

The ability of RITRACKS to calculate dose was tested by comparing the calculated total dose to a spherical target, based on the total energy deposited within the simulated sphere by RITRACKS, to the expected total dose to a spherical target from the simulated fluence of  $1000 \text{ MeV nucleon}^{-1}$  ions. Calculated total dose to a

target, in Gy, is related to the energy absorbed per unit mass, generally in joules per kilogram. Based on the final output units of RITRACKS, and using the fact that mass of the target is equal to the product of the target's density ( $\rho_t$ ) and volume ( $V_t$ ),  $D_{calc}$  can be expressed as

$$D_{calc} = \frac{E_{abs}}{\rho_t \cdot V_t}, \quad (3-1)$$

where  $E_{abs}$  is in units of MeV. Under the experimental parameters listed in Section II: Materials and Methods,  $D_{calc}$  for an irradiation volume diameter of 1.0  $\mu\text{m}$  under the Infinite Boundary condition in the homogenous system can be calculated as

$$D_{calc} = \frac{1.04 \times 10^3 \text{ MeV}}{1 \frac{\text{g}}{\text{cm}^3} (1.0 \mu\text{m})^3 \cdot \left(10^{-12} \frac{\text{cm}^3}{\mu\text{m}^3}\right)} \cdot 1.6 \times 10^{-10} \frac{\text{Gy}}{\text{MeV/g}} \approx 3.19 \times 10^5 \text{ Gy}, \quad (3-2)$$

The calculated total dose to a spherical target in RITRACKS based on total energy deposited in the target can be seen in Table 3-2. The same trends seen in this table as seen in Table 3-1 are expected due to the fact that the total dose calculations are based on the total energy deposited within the spherical target.

Table 3-2. Calculated Total Dose to Spherical Target (Gy)

Irradiation Volume diameter ( $\mu\text{m}$ )	Homogenous		Heterogeneous	
	Infinite Boundary	PBC Boundary	Infinite Boundary	PBC Boundary
d = 1.0	3.19E+05	4.27E+05	3.34E+05	4.92E+05
d = 1.05	3.21E+05	4.35E+05	3.48E+05	5.11E+05
d = 1.225	3.26E+05	4.48E+05	3.60E+05	5.40E+05
d = 1.414	3.25E+05	4.55E+05	3.66E+05	5.70E+05

The expected total dose in Grey (Gy),  $D_{exp}$ , can be calculated by

$$D_{exp} = \varphi \cdot \frac{LET}{\rho}, \quad (3-3)$$

where  $\varphi$  is the fluence of the incident beam in  $\text{cm}^{-2}$ , and  $LET/\rho$  is the mass stopping power of the incident ion in units of  $\text{MeV} \cdot \text{cm}^2 \text{g}^{-1}$  assuming charged particle equilibrium. Under the experimental parameters listed in Section II: Materials and Methods,  $D_{exp}$  is then

$$D_{exp} = \frac{15000 \text{ particles}}{\frac{\pi}{4} \cdot (1.0 \text{ } \mu\text{m})^2 \cdot (10^{-8} \frac{\text{cm}^2}{\mu\text{m}^2})} \cdot 1492.4 \frac{\text{MeV} \cdot \text{cm}^2}{\text{g}} \cdot 1.6 \times 10^{-10} \frac{\text{Gy}}{\text{MeV/g}} \approx 4.56 \times 10^5 \text{ Gy}. \quad (3-3)$$

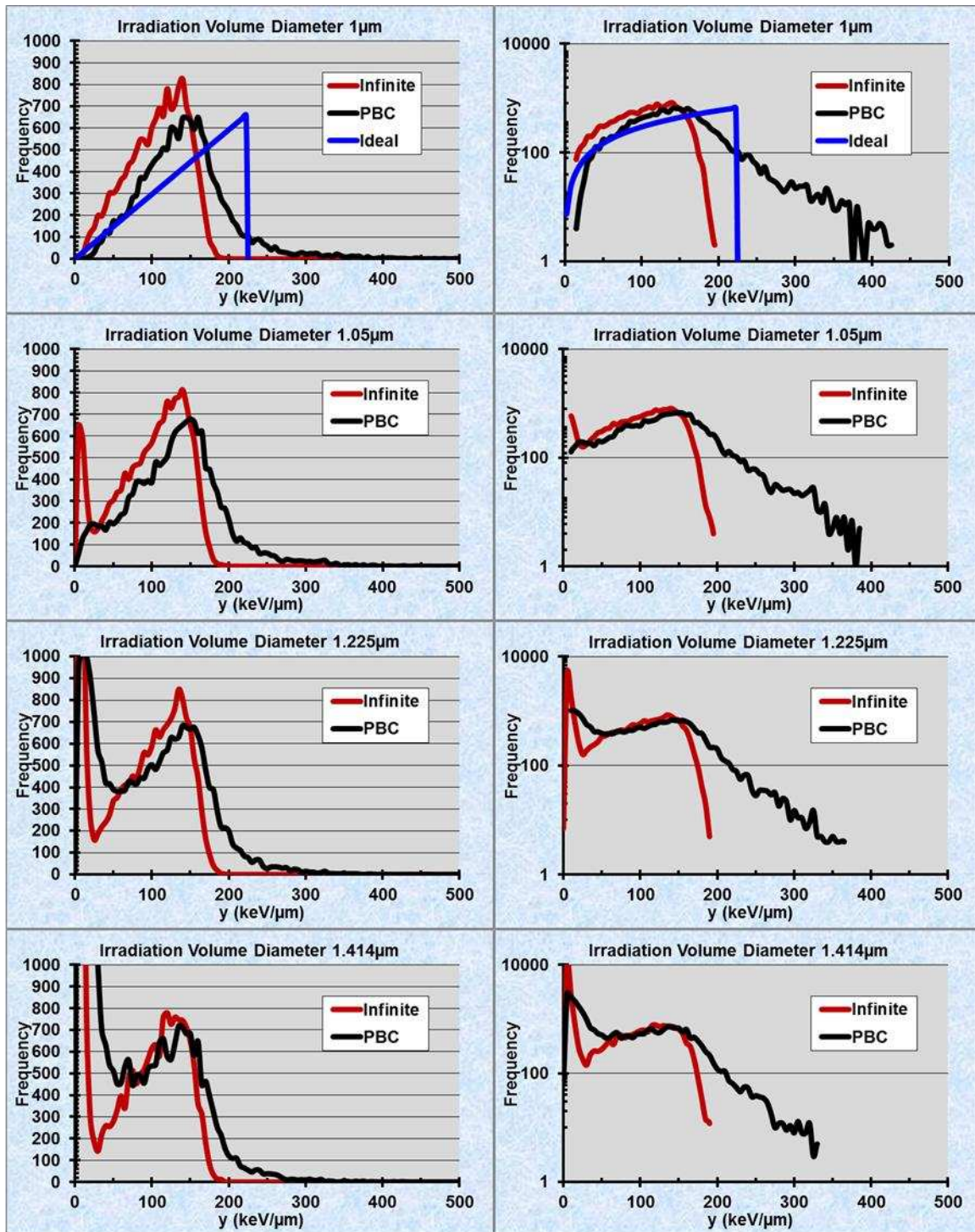
A comparison of the calculated dose from RITRACKS and the expected dose can be seen in Table 3-3. This table shows the ratio of the dose calculation from RITRACKS to the expected dose. When the Infinite Boundary setting is used, RITRACKS achieves approximately 70% of the expected dose in the homogenous system and approximately 80% of the expected dose in the heterogeneous system. Under the Periodic Boundary setting in the homogenous system, the calculated dose ranges from 94-100% of the expected dose. In the heterogeneous system, utilization of the Periodic Boundary setting overestimates the expected dose for all irradiation volume diameters.

Table 3-3. Ratio of Dose Calculated from RITRACKS to Expected Dose

Irradiation Volume diameter ( $\mu\text{m}$ )	Homogenous		Heterogenous	
	Infinite Boundary	PBC Boundary	Infinite Boundary	PBC Boundary
d = 1.0	0.70	0.94	0.73	1.08
d = 1.05	0.70	0.95	0.76	1.12
d = 1.225	0.71	0.98	0.79	1.18
d = 1.414	0.71	1.00	0.80	1.25

*Patterns of Energy Deposition in RITRACKS*

The distributions of energy deposition events for these experiments, in units of lineal energy, are shown in Figures 3-1 and 3-2 for the homogenous and heterogeneous cases, respectively. The distributions for the irradiation volume diameter of 1.0  $\mu\text{m}$  were compared to a computations using  $f(\epsilon)$  assuming  $\epsilon = LET \cdot \text{pathlength}$ , where pathlength represents the trajectory of the incident particle through the TEPC cavity. Under this assumption, no radial energy loss from secondary electrons is expected, no contribution from forward moving secondary electrons exists, and energy transfer to the medium is expressed as a single point along the pathlength of the primary ion. If each trajectory is a straight line, the trajectories are represented by secants or chords through the spherical volume. For this Ideal Case, where the chords are distributed by the intersection of  $\mu$ -random incident particles,  $\bar{y}_f = LET$  and  $\bar{y}_D = 9/8 LET$ . (Note: due to spherical symmetry, a  $\mu$ -random distribution of chords is obtained with a uniform plane parallel beam). In all irradiation volume diameter cases, utilizing the Periodic Boundary setting shifts the distribution towards higher energy events.



**Figure 3-1.** Energy deposition distributions for irradiation volume diameters of 1, 1.05, 1.225, and 1.414  $\mu\text{m}$  for the homogenous case. Linear-linear (*left*) and Logarithmic-linear (*right*) graphs of the data are shown. Infinite and Periodic Boundary (PBC) Settings are plotted. The Ideal Case, when no radial energy loss is expected, is also shown.

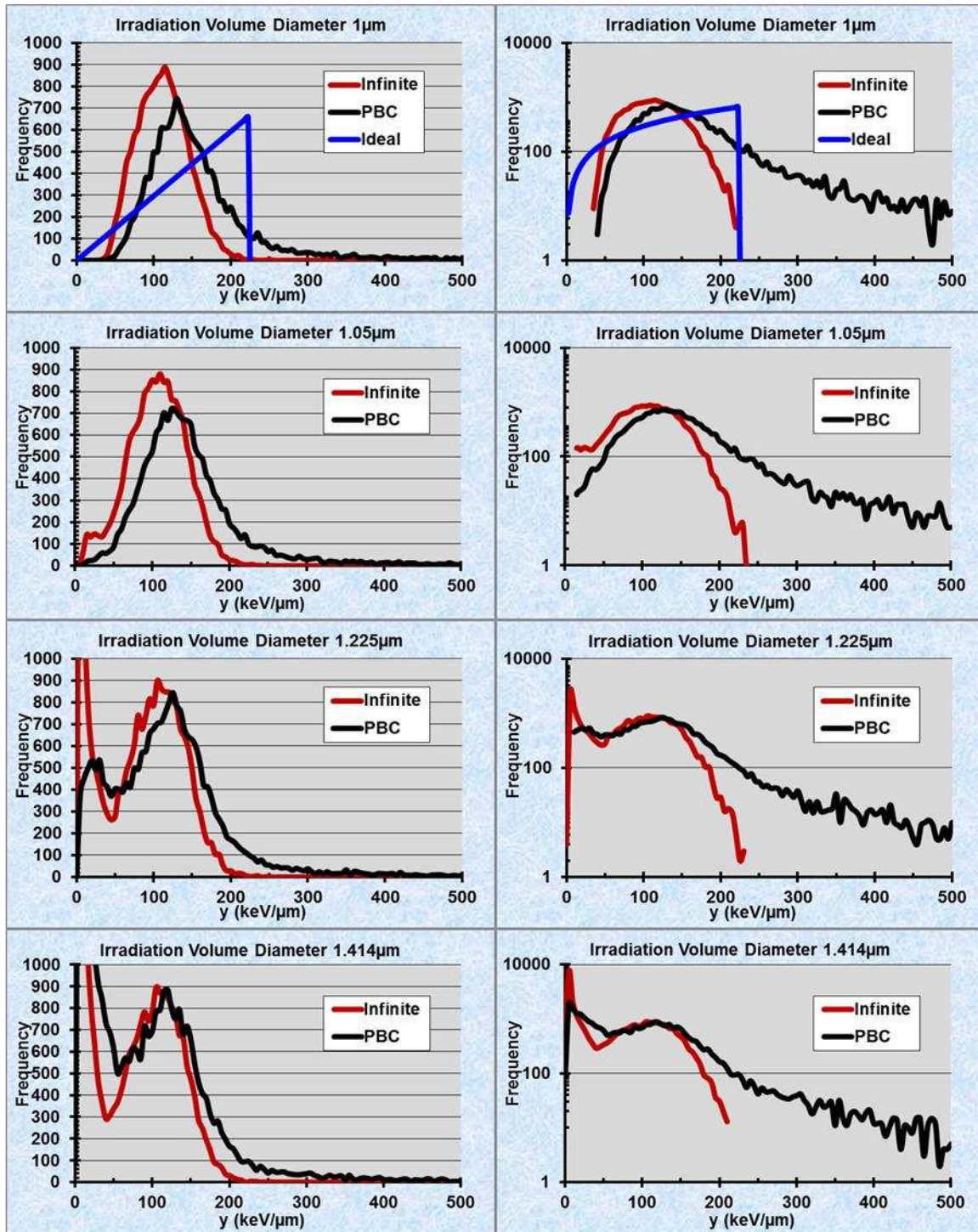


**Figure 3-2.** Energy deposition distributions for irradiation volume diameters of 1, 1.05, 1.225, and 1.414  $\mu\text{m}$  for the heterogeneous case. Linear-linear (*left*) and Logarithmic-linear (*right*) graphs of the data are shown. Infinite and Periodic Boundary (PBC) Settings are plotted. The Ideal Case, when no radial energy loss is expected, is also shown.

The data from Figures 3-1 and 3-2 were used to determine  $\bar{y}_f$  and  $\bar{y}_D$  for Fe particles at 1000 Mev nucleon<sup>-1</sup>. Tables 3-4 and 3-5 provide a summary of the results, including the TEPC data from Rademacher *et al.* and the Ideal Case. The homogenous system simulation nearest this assumption, for both the frequency mean lineal energy and the dose mean lineal energy, is seen when using the Periodic Boundary setting with an irradiation diameter of 1.0  $\mu\text{m}$ . The simulations nearest the experimental TEPC  $\bar{y}_f$  and  $\bar{y}_D$  are observed using the Periodic Boundary setting with 1.414 ( $\bar{y}_f$ ) and 1.225 ( $\bar{y}_D$ )  $\mu\text{m}$  irradiation volume diameters. The heterogeneous system results do not yield the same relationships and there appears to be no optimal RITRACKS simulation setting that best calculated both  $\bar{y}_f$  and  $\bar{y}_D$  for the TEPC and for the Ideal Case.

Table 3-4.  $\bar{y}_f$  and  $\bar{y}_D$  for the Homogenous Cases Under the Infinite (INF) and Periodic Boundary (PBC) Settings (keV  $\mu\text{m}^{-1}$ )

Volume Diameter ( $\mu\text{m}$ )	1.0		1.05		1.225		1.414		TEPC Data	Ideal Case
	INF	PBC	INF	PBC	INF	PBC	INF	PBC		
$\bar{y}_f$	105	140	96	129	71	98	53	75	79	150
$\bar{y}_D$	118	164	118	158	117	143	115	132	143	169

Table 3-5.  $\bar{y}_f$  and  $\bar{y}_D$  for the Heterogeneous Cases Under the Infinite (INF) and Periodic Boundary (PBC) Settings (keV  $\mu\text{m}^{-1}$ )

Volume Diameter ( $\mu\text{m}$ )	1.0		1.05		1.225		1.414		TEPC Data	Ideal Case
	INF	PBC	INF	PBC	INF	PBC	INF	PBC		
$\bar{y}_f$	109	161	104	152	79	118	60	93	79	150
$\bar{y}_D$	119	215	117	210	113	181	112	165	143	169

### *Comparison of RITRACKS and TEPC Patterns of Energy Deposition*

RITRACKS patterns of energy deposition for both the homogenous and heterogeneous systems under Infinite and Periodic Boundary settings were compared

to the distribution from the previous TEPC experiment by overlaying normalized data on the same frequency distribution graph, seen in Figures 3-3 and 3-4. In the homogenous system, the Infinite Boundary setting yields a distribution shape similar to the TEPC but the peak frequency energies are lower than expected. The PBC setting gives frequency distribution energy ranges comparable to those reported by the TEPC, but the distribution is skewed towards lower energy events. In the heterogeneous system, the Infinite Boundary setting generates distributions with peak frequency energies approximately  $40 \text{ keV } \mu\text{m}^{-1}$  less than the peak energy seen in the TEPC distribution. The Periodic Boundary setting displays a distribution similar to the Infinite Boundary homogenous system distribution, with the exception that there are markedly fewer events occurring at  $<50 \text{ keV } \mu\text{m}^{-1}$ .

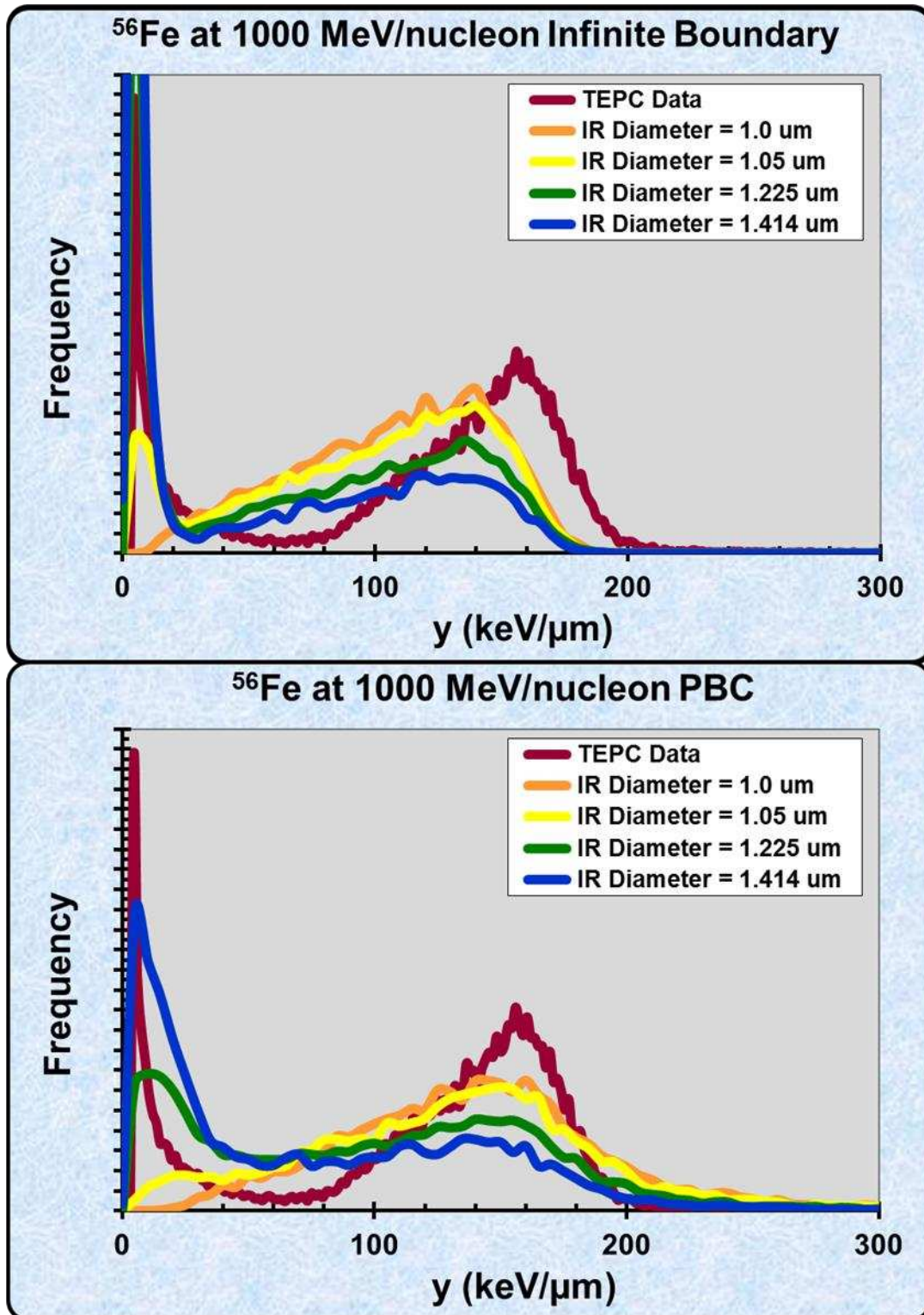


**Figure 3-3.** Energy deposition distributions for the homogenous cases under the Infinite (*top*) and Periodic Boundary (PBC) Settings compared to TEPC data from Rademacher *et al.* The four irradiation volume diameters (IR Diameter) used in RITRACKS experiments are included.

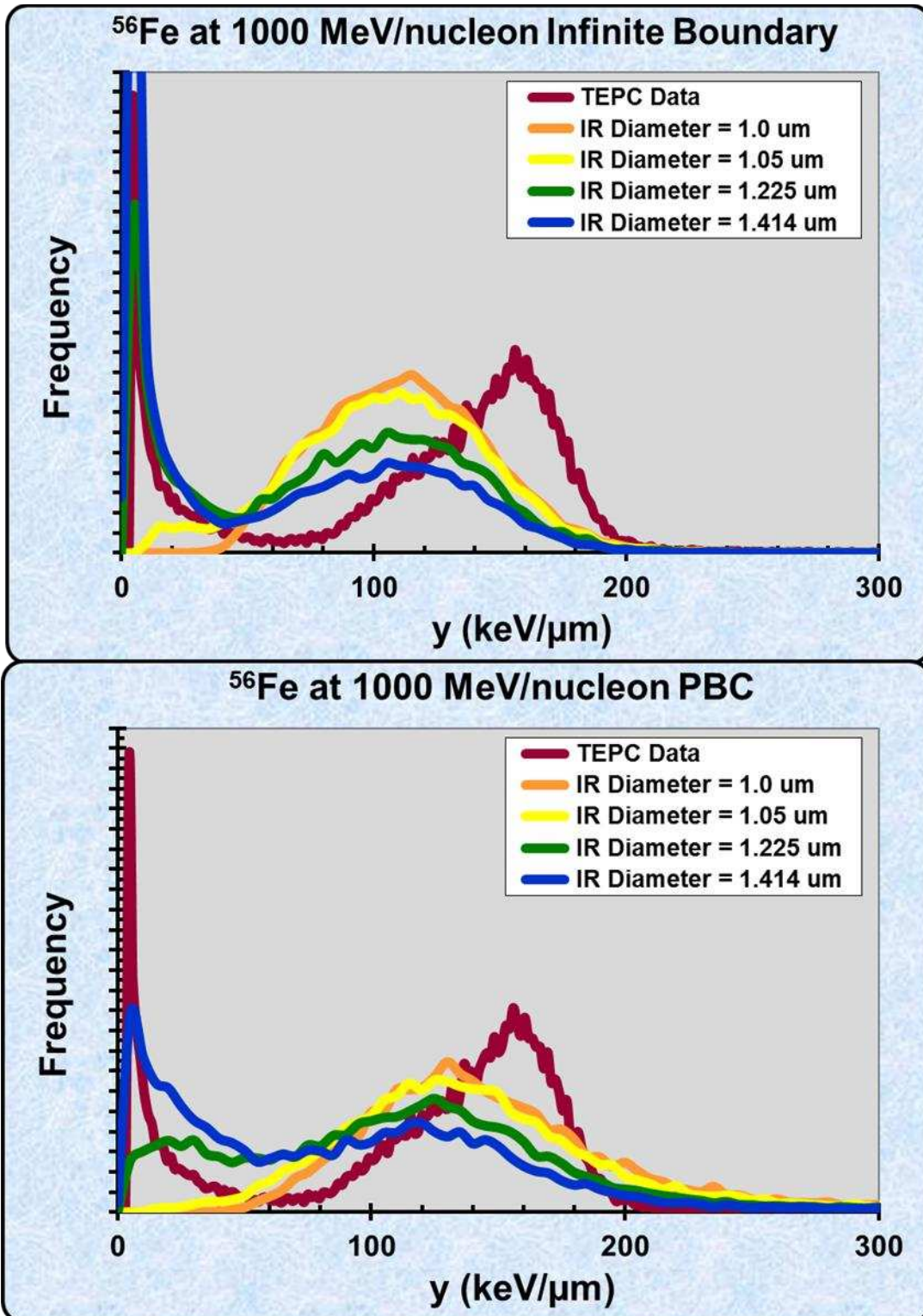


**Figure 3-4.** Energy deposition distributions for the heterogeneous cases under the Infinite (*top*) and Periodic Boundary (PBC) Settings compared to TEPC data from Rademacher *et al.* The four irradiation volume diameters (IR Diameter) used in RITRACKS experiments are included.

## DISCUSSION

The purpose of these computations was to test the capabilities of RITRACKS by computing energy deposition (i.e., absorbed dose) in spherical volumes with diameters of 1  $\mu\text{m}$  and compare patterns of energy deposition between RITRACKS and previous measurements using a TEPC. Initially, the extension of RITRACKS into the microdosimetric range was meant to verify the energy deposition distribution patterns observed in the TEPC. Borak *et al.* reported that the TEPC correctly measured absorbed dose for uniform beams of specific ions when including all events in the distribution similar to Figure 2-1 in the final calculation. It was concluded that Charged Particle Equilibrium (CPE) was achieved when using a tissue equivalent walled TEPC with a thickness of 2.54 mm. By definition, "CPE exists for a volume if each charged particle of a given type and energy leaving the volume is replaced by an identical particle of the same energy entering, in terms of the expected values" (Turner, 2007). The first step in benchmarking RITRACKS was then to prove it could calculate absorbed dose as effectively as the TEPC.

Earlier versions of RITRACKS only possessed the Infinite Boundary setting. Even though there were specified irradiation volume parameters, having an Infinite Boundary condition meant that all generated delta rays were free to interact as expected within an infinite uniformly dense medium. As seen in Table 3-3, using the Infinite Boundary setting provided approximately 70% of the expected dose in the homogenous system and 80% of the expected dose in the heterogeneous system. Secondary electrons from a  $1000 \text{ MeV nucleon}^{-1}$  Fe ion have a wide distribution of CSDA ranges in liquid water, and in some cases larger than the one micron diameter

spherical target used in the simulation. Rademacher *et al.* reported that approximately 70-75% of the energy deposited in the target by a uniform 1000 MeV nucleon<sup>-1</sup> Fe ion beam was attributed to the primary ion directly interacting with the sensitive volume. The discrepancy in dose was therefore attributed to the fact that RITRACKS was not attaining CPE. One could pose to expand the target's dimensions in RITRACKS so that any generated secondary electron would have a higher probability of interaction and energy deposition within the target. This would defeat the purpose of simulating volumes similar to mammalian cells, and the resulting energy deposition distributions would be incorrect with regards to the desired dimensions.

Due to this discrepancy, the PBC setting was introduced as a way to ensure the high energy delta rays escaping the volume of interest would deposit all of their energy locally. The PBC setting makes it so all energy is deposited within the irradiation volume, regardless of the target volume's dimensions. Table 3-3 shows this incorporation in the homogenous system yielded the desired expected dose, but only under a certain irradiation volume to target volume ratio in RITRACKS. When the irradiation volume diameter equaled the diameter of the target, 94% of the expected dose was calculated. Approximately 100% of the expected dose is not achieved until the diameter of the irradiation volume is such that 50% of the incident ions are estimated to not directly interact with the target. A histogram comparison of these dose results can be seen in Figure 4-1.

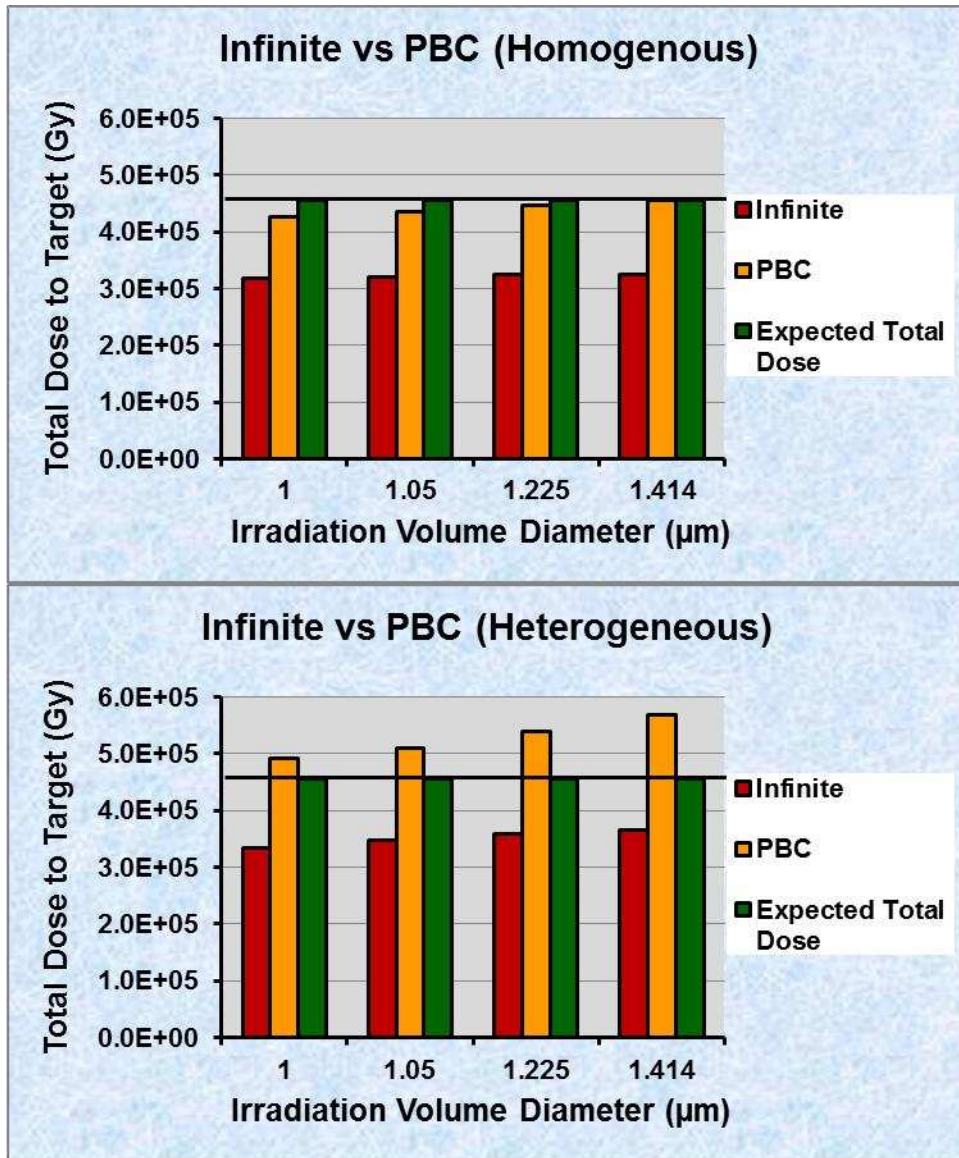


**Figure 4-1.** Histogram comparison of total dose to the spherical target in RITRACKS per irradiation volume diameter. The Infinite and Periodic Boundary settings are contrasted in the homogenous (*top*) and heterogeneous (*bottom*) systems.

It is possible that the trends in Table 3-3 and Figure 4-1 for the PBC setting could be attributed to the ion ( $Z$ ) and velocity ( $\text{MeV nucleon}^{-1}$ ) of the incident ions, as well as the ratio of the irradiation volume to the target volume. Further tests would need to be performed to verify this correlation. In the heterogeneous system, the PBC setting causes the total calculated dose to the target to be larger than expected for all

irradiation volume diameters. This can be attributed to the fact that the nature of the PBC setting creates abnormally large energy deposition events as generated secondary electrons continually cycle through the irradiation volume and target. Results indicated each irradiation volume parameter initially chosen in this experiment should be considered when analyzing energy deposition distributions for RITRACKS.

Data used from the previous TEPC experiments were in units of lineal energy, therefore data simulated within RITRACKS was converted to lineal energy for comparison analysis. Tables 3-4 and 3-5 are a result of these conversions. Figure 4-2 displays a histogram comparison of the values from these tables.

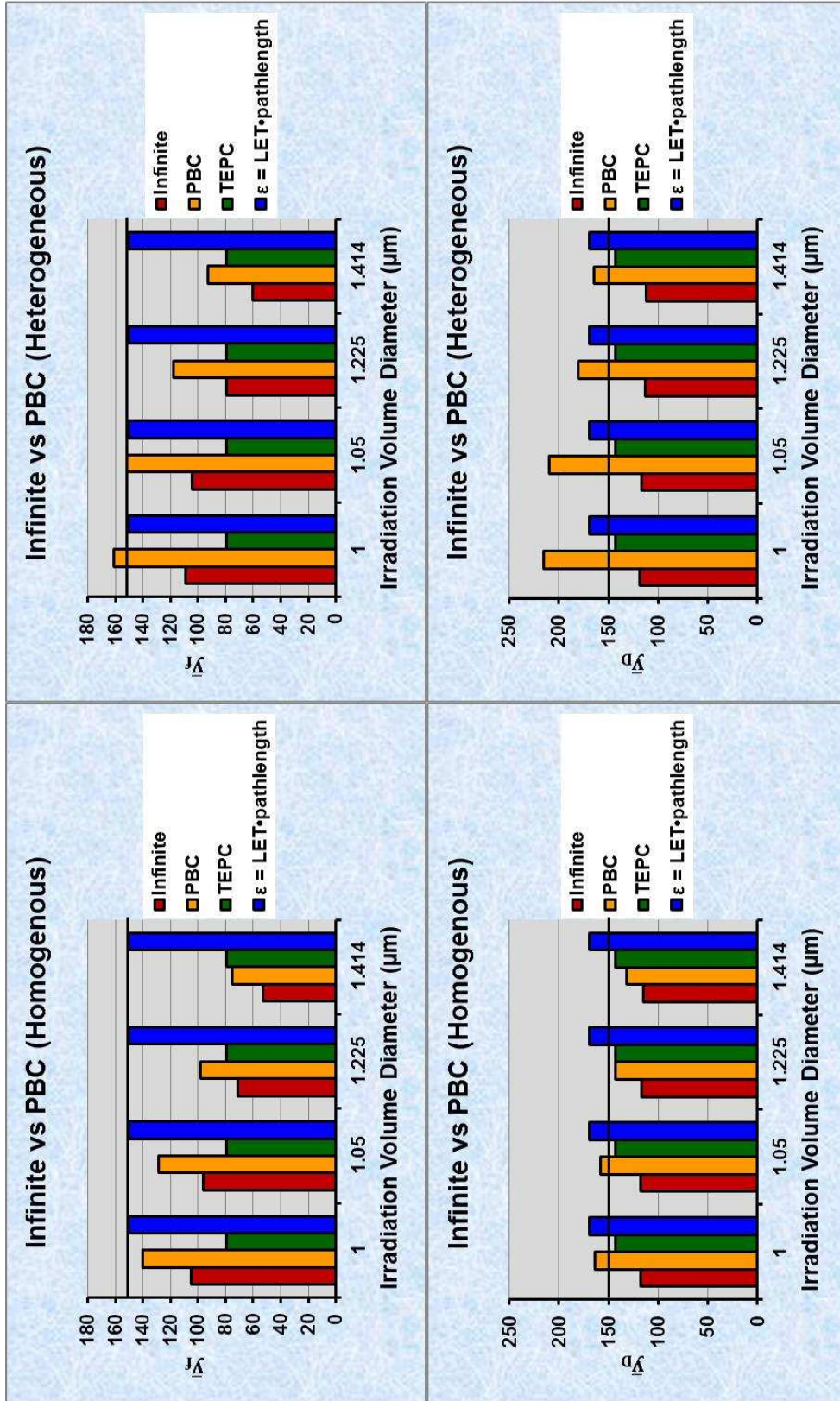


**Figure 4-2.** Histogram comparisons of the frequency mean lineal energy  $\bar{y}_f$  (top), and dose averaged lineal energy  $\bar{y}_D$  (bottom) in units of  $\text{keV } \mu\text{m}^{-1}$  per irradiation volume diameter between the Infinite and Periodic Boundary settings are shown. Data from the homogeneous and heterogeneous systems are shown. A line has been drawn across each graph as an indicator of expected LET. TEPC data and the  $\text{LET} \cdot \text{pathlength}$  values were included for each irradiation volume diameter to aid comparison.

Tables 4-1 and 4-2 provide percent differences for these results. Within these tables, a positive percentage (+) corresponds to the RITRACKS calculation being that percentage larger than the compared value, while a negative percentage (-) corresponds to the RITRACKS calculation being that percentage less than the compared value. For example, in Table 4-1 for an irradiation volume diameter of 1.0, the Infinite Boundary setting in the homogenous system yielded a  $\bar{y}_f$  25% larger than the value calculated from the TEPC experiments and a  $\bar{y}_f$  43% smaller than the Ideal Case.

Table 4-1. RITRACKS Percent Differences from  $\bar{y}_f$  TEPC Results and the Ideal Case Under the Infinite (INF) and Periodic (PBC) Boundary Settings for the Homogenous and Heterogeneous Systems

Homogenous				
Volume Diameter ( $\mu\text{m}$ )	INF from TEPC	INF from Ideal Case	PBC from TEPC	PBC from Ideal Case
1.0	+25%	-43%	+44%	-7%
1.05	+18%	-56%	+39%	-16%
1.225	-11%	-111%	+19%	-53%
1.414	-49%	-183%	-5%	-100%
Heterogeneous				
Volume Diameter ( $\mu\text{m}$ )	INF from TEPC	INF from Ideal Case	PBC from TEPC	PBC from Ideal Case
1.0	+28%	-38%	+51%	+7%
1.05	+24%	-44%	+48%	+1%
1.225	0%	-90%	+33%	-27%
1.414	-32%	-150%	+15%	-61%

Note:  $\bar{y}_f$  TEPC data was 47% smaller (-47%) than  $\bar{y}_f$  Ideal Case

Table 4-2. RITRACKS Percent Differences from  $\bar{y}_D$  TEPC Results and the Ideal Case Under the Infinite (INF) and Periodic (PBC) Boundary Settings for the Homogenous and Heterogeneous Systems

Homogenous				
Volume Diameter ( $\mu\text{m}$ )	INF from TEPC	INF from Ideal Case	PBC from TEPC	PBC from Ideal Case
1.0	-21%	-43%	+13%	-3%
1.05	-21%	-43%	+9%	-7%
1.225	-22%	-44%	0%	-18%
1.414	-24%	-44%	-8%	-28%
Heterogeneous				
Volume Diameter ( $\mu\text{m}$ )	INF from TEPC	INF from Ideal Case	PBC from TEPC	PBC from Ideal Case
1.0	-20%	-42%	+33%	+21%
1.05	-22%	-44%	+32%	+20%
1.225	-27%	-50%	+21%	+7%
1.414	-28%	-51%	+13%	-2%

Note:  $\bar{y}_D$  TEPC data was 15% smaller (-15%) than  $\bar{y}_D$  Ideal Case

As the irradiation volume diameter expands for both boundary settings in the homogenous system, the increasing percent difference from the Ideal Case for  $\bar{y}_f$  and  $\bar{y}_D$  is due to the fact that the Ideal Case is a quantity corresponding to particles with no radial energy loss from delta rays. For each irradiation volume diameter expansion in RITRACKS, the primary incident ions have a higher probability of not directly interacting with the fixed-diameter target. Radial distribution of energy, or namely the energy deposited in the target by delta rays, becomes more important as the trajectory of the primary ion from the target increases because the dose delivered to the target will

heavily rely on these events. The Infinite Boundary setting is most influenced by this because CPE is not occurring; therefore the amount of delta rays generated within the medium that should deposit energy in the target is less than what is expected. In the case of the PBC setting, the effect is less pronounced, but it is clear that the setting is subject to the aforementioned ratio of the irradiation volume to the target volume. Comparing  $\bar{y}_f$  TEPC data with the Infinite Boundary setting follows a similar trend, with the exception that somewhere between an irradiation volume diameter of 1.05 and 1.225  $\mu\text{m}$  the Infinite Boundary setting switches from overestimating to underestimating TEPC data. A comparable transition occurs when comparing  $\bar{y}_f$  TEPC data with the Periodic Boundary setting, where the change from over to underestimation occurs between 1.225 and 1.414  $\mu\text{m}$ . When comparing the homogenous system to TEPC data  $\bar{y}_D$ , an inverse relationship exists between the two boundary settings. As the irradiation volume diameter increases, the percent difference between the Infinite Boundary and the TEPC increases while the Periodic Boundary draws closer to the TEPC data. All of these trends are also observed in the heterogeneous system, but the percent differences are all increased in value due to the fact that the heterogeneous energy deposition distributions display a distribution range with considerably larger energies when compared to the homogenous system.

Figure 3-3 shows the patterns of energy deposition in lineal energy for the four irradiation volume diameters in RITRACKS and experimental TEPC data under both boundary settings for the homogenous case. The same TEPC data set is used in both figures. As stated previously, the pattern seen for this data in the 100-200 keV  $\mu\text{m}^{-1}$  range is what would be expected when the trajectory of the primary ion directly passes

through the sensitive volume of the TEPC. The peak on the lower end of the distribution, between 5-30 keV  $\mu\text{m}^{-1}$ , is what would be expected when delta rays produced in the wall of the detector interact with the sensitive volume. Comparing these expectations to the Infinite Boundary setting in Figure 3-3, it can be seen that this setting shifts the distributions towards lower energy events. A tendency towards lower energies was expected considering the Infinite Boundary setting underestimated expected dose by approximately 30%. In the case where the irradiation volume diameter is equal to the spherical target diameter (1  $\mu\text{m}$ ), all events resulted from the trajectory of the primary ion passing through the target. The frequency-mean lineal energy for this case is larger than the TEPC data, but the peak frequency energy for the data is approximately 20 keV  $\mu\text{m}^{-1}$  less than the TEPC distribution. The distribution generated by RITRACKS also has a higher frequency of events not seen in the TEPC (between 30 and 100 keV  $\mu\text{m}^{-1}$ ). RITRACKS displays this distribution because there is a detriment in the contribution from secondary electrons for total energy deposited per primary ion simulation, resulting in energy deposition events mainly influenced by the possible track lengths the primary ion can possess in the spherical target. As the irradiation volume diameter is expanded in RITRACKS simulations, more lower-energy events result because it is possible for the trajectory of the primary ion to not directly pass through the target. Effectively, the distributions begin to tend towards the relatively low energy delta ray interactions and away from the higher energy primary ion interactions within the target.

Utilization of the PBC setting shifts the distributions towards the TEPC energy range, seen in Figure 3-3. While this shift towards higher energies yields the

approximate expected dose, the frequency distribution does not resemble the TEPC data. In every RITRACKS simulation, the PBC setting ensures no energy escapes the irradiation volume, resulting in a broader spectrum of energy events when compared to TEPC data and data from the Infinite Boundary setting (Figure 3-1). The broader spectrum is a consequence of how the PBC functions. Any delta ray that would normally escape the volume in the Infinite Boundary setting continues to “cycle” through the irradiation volume, yielding a wide variation of trajectories and energy deposition events until it reaches a certain threshold. In the TEPC setting, these delta ray energies for a 1000 MeV nucleon<sup>-1</sup> <sup>56</sup>Fe ion would not be expected due to the nature of the interactions with the wall of the TEPC.

Stated previously, the TEPC correctly measured absorbed dose when integrating over all events within the TEPC distribution used for the comparison with RITRACKS, implying that CPE was attained under the set experimental parameters. It is assumed that the TEPC distribution is what is expected for a 1 μm cellular target within a biological system. TEPC retains a tissue equivalent gas and wall, and the relationship between density and diameter can be determined such that TEPC dimensions are approximately equal to a 1 μm cellular target. The interactions observed and the resulting energy deposition events recorded by the TEPC have been attributed to the vast density difference between the wall and the sensitive gas of the detector. Previous TEPC data analysis showed that, for impact parameters less than the radius of the sensitive gas volume, the approximate ratio of  $\bar{y}_f$  of the TEPC response to the expected *LET* for that specific ion and energy was 0.8, i.e. approximately 80% of the expected *LET* was observed when measuring energy imparted within the gas of the TEPC for

those impact parameters. When including the contribution from events where the impact parameter was greater than or equal to the radius of the sensitive gas,  $\bar{y}_f$  of the TEPC approximated *LET*. If  $\bar{y}_f$  is equal to expected *LET*, then the correct absorbed dose is calculated within the TEPC, leading to the conclusion that the distribution resulting from the wall of the TEPC could be what is actually happening on the microdosimetric level for HZE particles and living cells. According to Fano's Theorem, "In a medium of given composition exposed to a uniform flux of primary radiation, the flux of secondary radiation is also uniform and independent of the density of the medium as well as the density variation from point to point" (Spencer, 1975). Essentially, the TEPC response and subsequent distributions would result regardless of the density difference in a uniform system, and the wall of the TEPC is simulating the secondary electron contribution from "tissue" surrounding the 1  $\mu\text{m}$  "cell."

The effects of varying density mediums on patterns of energy deposition were also tested in RITRACKS. In the heterogeneous case, the density of the target was one tenth that of the density of the surrounding medium. Due to the limitations of RITRACKS at this time, no larger difference in density between the target and irradiation volume was studied. The same relationships seen between the Infinite and Periodic Boundary settings in the homogenous case were observed. Referring to Tables 3-1 and 3-2, utilization of a heterogeneous density system leads to an increase in total energy deposited within the target and subsequent calculated total dose to the target. The ratio of the total calculated dose to the total expected dose (Table 3-3) also increases, to a point where RITRACKS consistently over-calculates dose using the Periodic Boundary setting. This can be explained by contrasting the patterns of energy

deposition between the homogenous and heterogeneous cases in Figures 3-1 and 3-2. Compared to the homogenous system, the heterogeneous system distributions display lower frequencies in the  $<50 \text{ keV } \mu\text{m}^{-1}$  range, as well as more events occurring within their respective peak frequency ranges. Effectively, the heterogeneous system  $\bar{y}_f$  becomes larger in value than the homogenous system  $\bar{y}_f$  for each irradiation volume diameter under both boundary settings. It can also be seen that the heterogeneous system has peak frequencies approximately  $25 \text{ keV } \mu\text{m}^{-1}$  less than their homogenous counterparts when comparing the two figures, but each heterogeneous system irradiation volume diameter lineal energy distribution possesses more events occurring in the higher energy range ( $>175 \text{ keV } \mu\text{m}^{-1}$ ).

Noticeable changes in  $\bar{y}_f$  and  $\bar{y}_D$  are observed between the 1.05 and 1.225  $\mu\text{m}$  irradiation diameters. Essentially, the impact of the primary ion not directly interacting with the target is being observed. These impacts are governed by the same reasons stated in the homogenous case, with the exception of being more pronounced due to the difference in densities.

## CONCLUSION

Computations were performed to benchmark calculations performed by the Monte Carlo code RITRACKS v3.07 with the response of spherical TEPCs to Fe particles at  $1000 \text{ MeV nucleon}^{-1}$ . The objective was to determine if data collected from RITRACKS v3.07 was comparable to the data collected from TEPC experiments performed in previous experiments. Analyses of total dose to a target, patterns of energy deposition, and effects of homogenous versus heterogeneous systems were conducted.

The data indicated that RITRACKS with an Infinite Boundary setting calculated between 70-80% of the expected dose. Secondary electrons were escaping the simulation volume and charged particle equilibrium was not occurring. Implementation of the Periodic Boundary setting yielded approximately 100% of the expected dose in the homogenous system, and an overestimation of expected dose was observed in the heterogeneous system. While the Periodic Boundary setting produced the expected dose under charged particle equilibrium, it is clear that this outcome relies upon the ratio of the irradiation volume to the target volume.

Computations were conducted using a previous version of RITRACKS to observe if the deficit in dose using the Infinite Boundary setting was due to using this particular ion and energy. The experiment tested the energy deposited in a cylindrical target with a length of 1 micron for  $100$  and  $400 \text{ MeV nucleon}^{-1}$  carbon ions and  $558 \text{ MeV nucleon}^{-1}$  neon ions. The diameters of the cylindrical targets increased from 100 nm to 2000 nm in 100 nm diameter intervals, each cylindrical target was centered radially and parallel to the trajectory of the incident primary ion. The primary ion had a track length of  $12 \mu\text{m}$ .

The center of the target was located 10.5  $\mu\text{m}$  from the point where the primary ion track originated. The simulation is depicted in Figure 5-1.

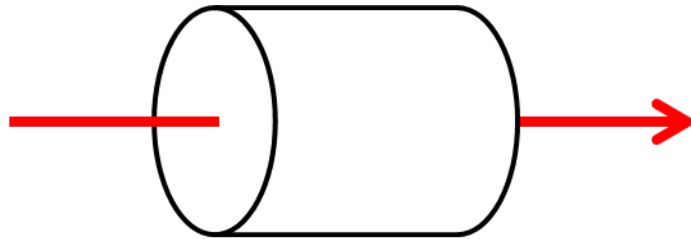


**Figure 5-1.** Drawing of Percent of LET computation study. The cylindrical target is center upon the primary ion beam (red arrow). Cylinder diameters ranging from 100 to 2000 nanometers were used to observe the radial distribution of LET in RITRACKS.

In theory, the energy deposited within the cylinder would serve as a surrogate for *LET* assuming charged particle equilibrium. The energy deposited in the targets was compared to the expected *LET* for the two ions with their respective energies. The ratio of RITRACKS calculations versus the expected *LET* can be seen in Figure 5-2.

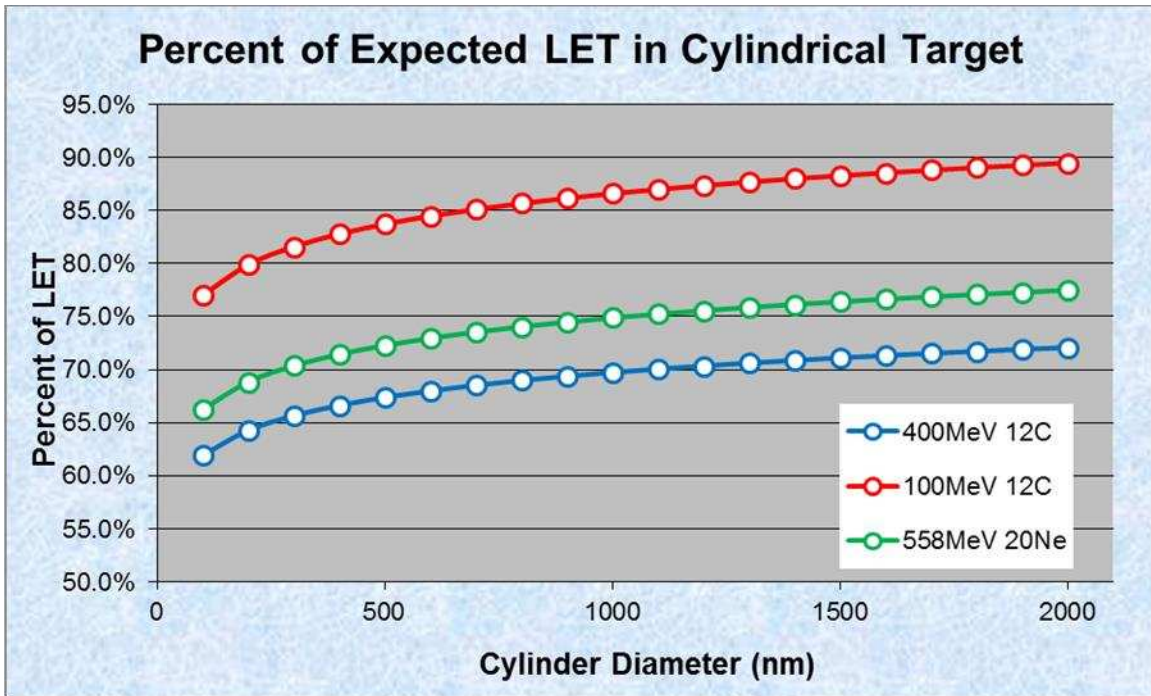


**Figure 5-2.** Percent of LET in cylindrical targets with expanding diameters for 100 and 400 MeV nucleon<sup>-1</sup> C ions and 558 MeV nucleon<sup>-1</sup> Ne ions. Diameters were expanded out to 2000 nm (2 μm).

In all of the simulations, the Infinite Boundary setting was used in a homogenous system. None of the simulations reached 100% of the expected *LET*. The closest approximation of *LET* for the test ions was 100 MeV nucleon<sup>-1</sup> <sup>12</sup>C. It should be noted that the *LET* of 100 MeV nucleon<sup>-1</sup> <sup>12</sup>C and 558 MeV nucleon<sup>-1</sup> <sup>20</sup>Ne are equal (approx. 26.2 keV μm<sup>-1</sup>). It was concluded that the specific ion and *LET* do not have as large an impact on the radial distribution of energy as the energy per nucleon of the primary ion in RITRACKS. As the energy of the ion increases, the distribution of possible secondary electron energies extends to larger ranges, yielding a higher probability of the secondary electrons escaping the irradiation volume and not contributing to the total energy deposition within the target.

In the homogenous system, the Infinite Boundary setting yields patterns of energy deposition similar to the TEPC, but have lower energies ranges for the distinct

regions described in Figure 2-1. The Periodic Boundary setting yields correct energy ranges for these distinct regions, but the frequencies for these events are dissimilar from the TEPC distribution. In the heterogeneous system, the Infinite Boundary setting generates distributions where the distinct regions are approximately  $40 \text{ keV } \mu\text{m}^{-1}$  less than those seen in the TEPC distribution. The Periodic Boundary heterogeneous system possess a distribution similar to the Infinite Boundary homogenous system distribution, with the exception that there are markedly fewer events occurring at  $<50 \text{ keV } \mu\text{m}^{-1}$ .

RITRACKS with the Periodic Boundary setting can give the correct dose under specific conditions, but it is not generating a similar distribution of energy deposition seen in experimental TEPC data. Obtaining the correct distribution of energy deposition is important when considering exposures to biological systems. When the primary ion directly interacts with the target, peak frequency energies exist between 100-200 keV, energies where a mammalian cell would die from exposure. The lower energy events however would not induce cell death and could induce mutations leading to carcinogenesis. Figure 5-3 transforms the distributions of lineal energy from Figures 3-3 and 3-4 to Specific Energy Imparted,  $z$ , in units of Gray (Gy) to better illustrate this point.

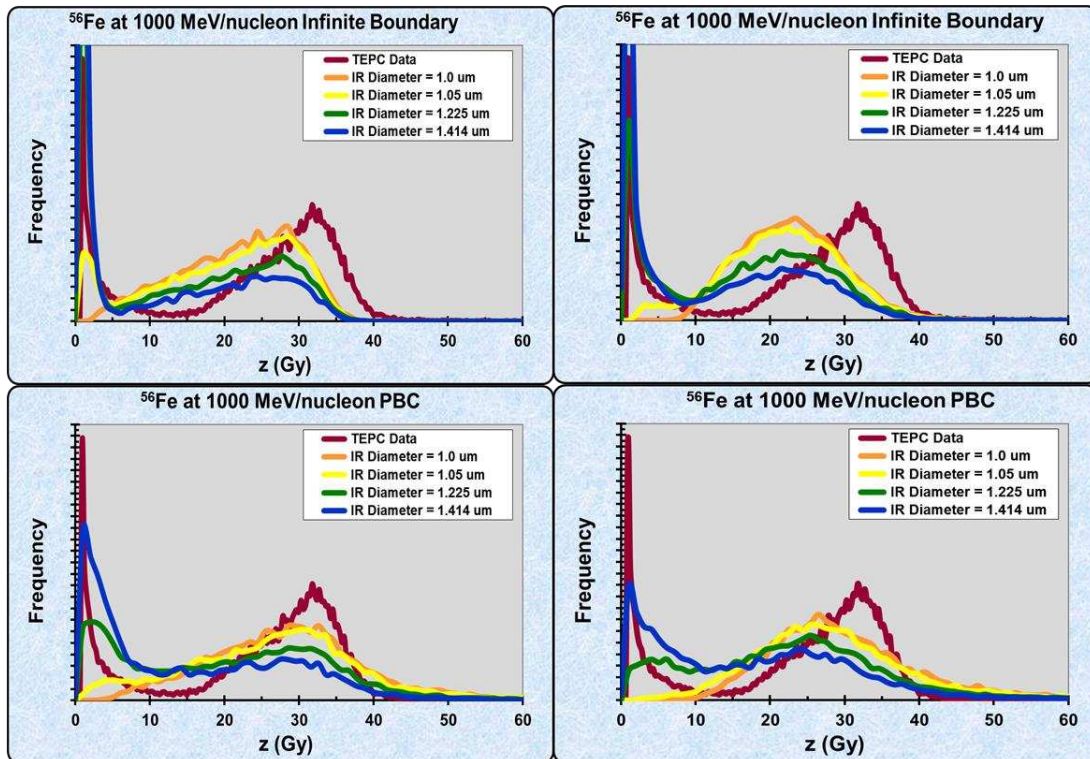


**Figure 5-3.** Specific Energy Imparted ( $z$ ) frequency distributions in units of Gy under the Infinite Boundary (*top*) and Periodic Boundary (*bottom*) settings for the homogenous (*left*) and heterogeneous (*right*) systems.

Doses in the region greater than 30 Gy are from energy deposition events where the incident particle intercepts the target are generally sufficient to result in cell mortality.

Doses in the region less than 5 Gy are from energy deposition events where the incident particle does not intercept the target. This region of events are important when considering RBE for HZE ions, making the generation of the correct energy deposition distribution in any radiation transport code essential for future experiments in the radiological field.

Risk, or the probability of occurrence of a harmful effect, is dependent upon the dose and the quality of the radiation, where quality can be assessed using lineal energy. RITRACKS v3.07 calculations of dose and  $\bar{y}_f$  are inconsistent among various settings (Infinite versus PBC, homogenous versus heterogeneous), and the patterns of energy

deposition yielding these calculations are dissimilar from distributions seen in an experimental TEPC. Correct calculations of dose and  $\bar{y}_f$  by RITRACKS based on known *LETs* can be achieved only under specific parameters and settings within the code, limiting the ability of RITRACKS v3.07 to properly assess damage to a biological system and the resulting risk at this time.

## REFERENCES

Ballarini, F., Alloni, D., Facchetti, A. & Ottolenghi, A., 2008. Heavy-ion effects: from track structure to DNA and chromosome damage. *New Journal of Physics*, Volume 10:075008.

Cucinotta, F. A., Nikjoo, H. & Goodhead, D. T., 2000. Model for radial dependence of frequency distributions for energy imparted in nanometer volumes from HZE particles. *Radiation Research*, Volume 153, pp. 459-468.

Dingfelder, M., 2006. Track structure: time evolution from physics to chemistry. *Radiation Protection Dosimetry*, Volume 122, pp. 16-21.

Gersey, B. B., 2006. *The Response of a Spherical Tissue-Equivalent Proportional Counter to Iron Particles from 200-1000 MeV/nucleon*, Ph.D. thesis, Fort Collins, CO: Colorado State University.

Gersey, B. B. et al., 2002. The response of a spherical tissue-equivalent proportional counter to Fe-56 particles from 200-1000 MeV/nucleon. *Radiation Research*, Volume 157, pp. 350-360.

Goodhead, D. T. & Nikjoo, H., 1989. Track structure analysis of ultrasoft X-rays compared to high- and low-LET radiations. *International Journal of Radiation Biology*, Volume 55, pp. 513-529.

Guetersloh, S. B., 2003. *Response of a Tissue Equivalent Proportional Counter to Different Ions Having a Similar Linear Energy Transfer*, Ph.D. thesis, Fort Collins, CO: Colorado State University.

Guetersloh, S. B. et al., 2004. The response of a spherical tissue-equivalent proportional counter to different ions having similar linear energy transfer. *Radiation Research*, Volume 161, pp. 64-71.

Hall, E., 1994. *Radiobiology for the Radiologist*. 4th ed. New York, NY: Lippincott-Raven.

ICRP, 1991. *Recommendations of the International Commission on Radiological Protection. Publication 60, International Commission on Radiological Protection, Annals of the ICRP.*, New York: Pergamon Press.

ICRP, 2003. *Relative Biological Effectiveness, Quality Factor, and Radiation Weighting Factor. Publication 92, International Commission on Radiological Protection, Annals of the ICRP*, New York: Pergamon Press.

ICRU, 1968. *Radiation Quantities and Units. Report 11, International Commission on Radiation Units and Measurements*, Washington, D.C.: s.n.

ICRU, 1983. *Microdosimetry. Report 36, International Commission on Radiation Units and Measurements*, Bethesda, MD: s.n.

Kellerer, A. M., 1971a. Considerations on the Random Traversal of Convex Bodies and Solutions for General Cylinders. *Radiation Research*, Volume 47, pp. 359-376.

Kellerer, A. M., 1971a. Considerations on the Random Traversal of Convex Bodies and Solutions for General Cylinders. *Radiation Research*, Volume 47, pp. 359-376.

Kellerer, A. M., 1971b. An assessment of wall effects in microdosimetric measurements. *Radiation Research*, Volume 47, p. 377.

Kellerer, A. M., 1971c. Event simultaneity in cavities. Theory of the distortions of energy deposition in proportional counters. *Radiation Research*, Volume 48, p. 216.

Lindborg, L., Hultqvist, M., Tedgren, A. C. & Nikjoo, H., 2013. Lineal energy and radiation quality in radiation therapy: model calculations and comparison with experiment. *Physics in Medicine and Biology*, Volume 58, pp. 3089-3105.

NCRP, 2002. *Operational Radiation Safety Program for Astronauts: A Basic Framework. Report Number 142, National Council on Radiation Protection and Measurements*, Bethesda, MD: s.n.

Nikjoo, H., O'Neill, P., Goodhead, D. T. & Terrissol, M., 1997. Computational modelling of low-energy electron-induced DNA damage by early physical and chemical events. *International Journal of Radiation Biology*, Volume 71, pp. 467-483.

Oldenburg, U. & Booz, J., 1970. Wall effects of the spherical counter. In: *Proceedings of the Second Symposium on Microdosimetry*. Brussels, Belgium: Commission of the European Communities, pp. 269, Report No. EUR 4452 (Ebert, H. G., Ed).

Plante, I. & Cucinotta, F. A., 2010. Calculations of the energy deposition and relative frequency of hits of cylindrical nanovolume in medium irradiated by ions by Monte-Carlo track structure simulations. *Radiation and Environmental Biophysics*, Volume 49, pp. 5-13.

Rademacher, S. E., 1997. *Wall Effects Observed in Tissue-Equivalent Proportional Counters, Ph.D. thesis*, Fort Collins, CO: Colorado State University.

Rademacher, S. E. et al., 1998. Wall Effects Observed in Tissue-Equivalent Proportional Counters from 1.05 GeV/nucleon Iron-56 Particles. *Radiation Research*, Volume 149, pp. 387-395.

Rossi, H. H., 1967. Energy distribution in the absorption of radiation. *Advances in Biological and Medical Physics*, Volume 11, p. 27.

Rossi, H. H. & Rosenzweig, 1955. A Device for the Measurement of Dose as a Function of Specific Ionization. *Radiology*, Volume 64, pp. 404-411.

Spencer, L. V., 1975. Some Comments on Fano's Theorem. *Radiation Research*, Volume 63, pp. 191-199.

Taddei, P. J., 2005. *The Response of a Spherical Tissue-Equivalent Proportional Counter to Different Heavy Ions with Similar Velocities*, Ph.D. thesis, Fort Collins, CO: Colorado State University.

Taddei, P. J. et al., 2006. The response of a spherical tissue-equivalent proportional counter to different heavy ions with similar velocities. *Radiation Measurements*, Volume 4179, pp. 1227-1234.

Taddei, P. J., Zhao, Z. & Borak, T. B., 2008. A comparison of the measured responses of a tissue-equivalent proportional counter to high energy heavy (HZE) particles and those simulated using the Geant4 Monte Carlo code. *Radiation Measurements*, Volume 43, pp. 1498-1505.

Turner, J. E., 2007. *Atoms, Radiation, and Radiation Protection*. 3rd ed. Oak Ridge, TN: Wiley-VCH.

Zirkle, R. E., Marchbank, D. F. & Kuck, K. D., 1952. Exponential and Sigmoid Survival Curves Resulting from Alpha and X-irradiation of *Aspergillus* spores. *Journal of Cellular Comparative Physiology*, 39(Supplement 1).